Polynomial $f(R)$ Palatini cosmology: Dynamical system approach

Marek Szydłowski*
Astronomical Observatory, Jagiellonian University, Orla 171, 30-244 Krakow, Poland and Mark Kac Complex Systems Research Centre, Jagiellonian University, Łojasiewicza 11, Krakow 30-348, Poland

Aleksander Stachowski†
Astronomical Observatory, Jagiellonian University, Orla 171, Krakow 30-244, Poland

(Received 16 December 2017; revised manuscript received 16 February 2018; published 23 May 2018)

We investigate cosmological dynamics based on $f(R)$ gravity in the Palatini formulation. In this study, we use the dynamical system methods. We show that the evolution of the Friedmann equation reduces to the form of the piecewise smooth dynamical system. This system is reduced to a 2D dynamical system of the Newtonian type. We demonstrate how the trajectories can be sewn to guarantee C^0 extendibility of the metric similarly as "Milne-like" Friedmann-Lemaître-Robertson-Walker spacetimes are C^0-extendible. We point out that importance of the dynamical system of the Newtonian type with nonsmooth right-hand sides in the context of Palatini cosmology. In this framework, we can investigate singularities which appear in the past and future of the cosmic evolution. We consider cosmological systems in both Einstein and Jordan frames. We show that at each frame the topological structures of phase space are different.

DOI: 10.1103/PhysRevD.97.103524

I. INTRODUCTION

Extended $f(R)$ gravity models [1–14] are intrinsic or geometric models of both dark matter and dark energy. Therefore, the idea of relational gravity, in which dark matter and dark energy can be interpreted as geometric objects, is naturally realized in $f(R)$ extended gravity.

The metric formulation of the extended gravity model gives the fourth order field equations, except for some cases, namely the Lovelock family of Lagrangians, where the field equations are second order [15]. This difficulty is solved by the Palatini formalism where the metric g and symmetric connection Γ are assumed to be independent variables. In this case, we get a system of second order partial differential equations [16]. This formalism also yields vacuum general relativity equations [17].

They are many papers about the Palatini formalism. In Olmo's paper [16], a review of the Palatini $f(R)$ theories appears. Papers [18,19] are about the scalar-tensor representation of the Palatini theories. Studies about the existence of nonsingular solutions in Palatini gravity are in [20,21]. The papers [22–26] are about black holes and their singularities in the Palatini approach. Studies about the choice of a conformal frame in the Palatini gravity are in [27,28]. Compact stars in the Starobinsky model are discussed in [29].

Conformal transformations became interesting after the formulation of Weyl's theory [30] aimed at unifying gravitation and electromagnetism. A conformally invariant version of special relativity was formulated in [31–33]. Another example of the development of Weyl's theory is the self-consistent, scale-invariant theory of Canuto *et al.* [34]. In this theory, the astronomical unit of length is related to the atomic unit by a scalar function which depends on the spacetime point. This theory contains a running cosmological "constant" $\Lambda(t) = \Lambda_0 \frac{t_0^2}{t^2}$.

Recently, the most significant and important achievements appear in the context of the understanding of the Palatini theory and their application to the cosmological problem description of the evolution of the Universe [1,12,16,35–38]. If we consider Friedmann-Robertson-Walker (FRW) cosmological models in the Palatini framework in the Einstein frame, one can obtain the exact formula for the running cosmological constant parameter [39].

Cosmology is the physics of the Universe but in opposition to the physical system; we do not know the initial conditions for the Universe. Therefore, to explain the current state of the Universe we consider all admissible physically initial conditions and study all evolutional paths for the evolution of the Universe in the universal cosmological time.

For this investigation of dynamics, the tools of the dynamical system theory are especially interesting. Dynamical system methods in the context of investigation dynamics of $f(R)$ gravity models have been used since Carroll [14,40]. The dynamical system is a system of

*marek.szydlowski@uj.edu.pl
†aleksander.stachowski@doctoral.uj.edu.pl

differential equations which describes the motion of the points in the phase space [41]. In this approach, the evolution of the Universe is represented by trajectories in the phase space (spaces of all states of the system at any time). The phase space is organized by the singular solution represented by critical points (points in which the derivative of solutions of the dynamical system is zero), invariant submanifolds (submanifolds which are invariant under the action of the dynamical system) and trajectories (geometrical representations of solutions of the dynamical system). Whole dynamics can be visualized in a geometrical way on the phase portrait—a phase space of all evolutional paths for all initial conditions [41]. We are looking for attractors (repellers) in the phase space to distinguish some generic evolution scenarios for the Universe [42].

We describe effectively the cosmic evolution in terms of the dynamical system of the Newtonian type. In this language, the motion of a fictitious particle mimics the evolution of the Universe and the potential contains all information needed for studying its dynamics. The right-hand side of the system cannot be a smooth function like for the cosmological evolution governed by general relativity. However, in any case, they are piecewise smooth functions. The context of the application of the Palatini formalism in the investigation of cosmological dynamics discovers the significance of new types of dynamical systems with nonsmooth right-hand sides [43]. It is interesting that cosmological singularities can be simply characterized in terms of the geometry of the potential $V(a)$, where a is the scale factor [43].

In this geometrical framework, singularities are manifested by a lack of analyticity of a potential itself or its derivatives with respect to the scale factor a and a diagram of the potential function (or its derivatives) possesses poles at some values of scale factor $a = a_{\rm sing}$. Because the potential function is an additive function of energy density components, the discontinuities appearing on a diagram of the potential $V(a)$ can be interpreted as a discontinuous jumping of a potential part. This idea that a potential form possesses some part which contains jump discontinuities can be applied in different cosmological contexts. For example, it was considered to characterize singularities in phantom cosmologies [44].

Finite late-time singularities can be classified into six categories according to divergences of physical characteristics [45,46]:

(a) Type 0: "Big crunch." The scale factor a is vanishing and the Hubble parameter H, effective energy density ρ and pressure p are blown up.
(b) Type I: "Big rip." The scale factor a, ρ and p are blown up. They are classified as strong [47,48].
(c) Type II: "Typical sudden." The scale factor a, ρ and H are finite, and $\dot{H}$ and p are divergent. Geodesics are not incomplete in this case [49–51].
(d) Type III: "Big freeze." The scale factor a is finite and H, ρ and p are blown up [49] or divergent [52]. In this case, there is no geodesic incompleteness and they can be classified as weak or strong [52].
(e) Type IV: "Generalized sudden." The scale factor a, H, ρ, p and $\dot{H}$ are finite but higher derivatives of the scale factor a diverge. These singularities are weak [53].
(f) Type V: "w singularities." The cosmological time t is finite, the scale factor a and ρ blow up, p vanishes and a coefficient of the equation of state $w = \frac{p}{\rho}$ diverges. These singularities are weak [54–56].

Following Królak [57], types 0 and I are strong, whereas types II, III and IV are weak singularities.

The main aim of the paper is a study of the cosmological equations based on $f(R)$ gravity in the Palatini formalism in both Einstein and Jordan frames. We want to show that the topological structures of phase space are different in these frames.

The order of this paper is as follows. In Sec. II, we introduce the Palatini formalism in the context of cosmology. We consider the Palatini formalism in cosmology in the Jordan frame in Sec. III and in the Einstein frame in Sec. IV. Section V is about differences between these frames. The last section is our conclusions.

II. PALATINI FORMALISM: INTRODUCTION

The Palatini gravity action of $f(\hat{R})$ gravity in the Jordan frame is given by

$$S = S_{\rm g} + S_{\rm m} = \frac{1}{2}\int \sqrt{-g} f(\hat{R}) d^4x + S_{\rm m}, \tag{1}$$

where $\hat{R} = g^{\mu\nu}\hat{R}_{\mu\nu}(\Gamma)$ is the Ricci scalar and $\hat{R}_{\mu\nu}(\Gamma)$ is the Ricci tensor of a torsionless connection Γ [16,58]. To simplify, we assume that $8\pi G = c = 1$.

After variation with respect to both dynamical variables g and Γ we obtain the field equations ($\delta S = 0$), which are the counterparts of the Einstein equations in the Palatini formalism, and an additional equation which establishes some relation between the metric and the connection,

$$f'(\hat{R})\hat{R}_{\mu\nu} - \frac{1}{2}f(\hat{R})g_{\mu\nu} = T_{\mu\nu}, \tag{2}$$

$$\hat{\nabla}_\alpha(\sqrt{-g}f'(\hat{R})g^{\mu\nu}) = 0, \tag{3}$$

where $T_{\mu\nu} = -\frac{2}{\sqrt{-g}}\frac{\delta L_{\rm m}}{\delta g_{\mu\nu}}$ is the matter energy momentum tensor and $\nabla^\mu T_{\mu\nu} = 0$ and $\hat{\nabla}_\alpha$ means that the covariant derivative is calculated with respect to connection Γ. The conservation equation $\nabla^\mu T_{\mu\nu} = 0$ is obtained from the Bianchi's identities $\nabla^\mu(f'(\hat{R})\hat{R}_{\mu\nu} - \frac{1}{2}f(\hat{R})g_{\mu\nu}) = 0$.

From the trace of the metric field equation (2), we get an additional equation, which is called the structural equation,

$$f'(\hat{R})\hat{R} - 2f(\hat{R}) = T, \tag{4}$$

where $T = g^{\mu\nu}T_{\mu\nu}$.

The metric g is the FRW metric for which the line element is given in the following form:

$$ds^2 = -dt^2 + a^2(t)\left[\frac{1}{1-kr^2}dr^2 + r^2(d\theta^2 + \sin^2\theta d\phi^2)\right], \tag{5}$$

where $a(t)$ is the scale factor, k is a constant of spatial curvature ($k = 0, \pm 1$) and t is the cosmological time.

In this paper, we assume perfect fluid with the energy-momentum tensor

$$T^{\mu}_{\nu} = \mathrm{diag}(-\rho, p, p, p), \tag{6}$$

where $p = w\rho$, $w = \mathrm{const}$ is a form of the equation of state. From the conservation equation $T^{\mu}_{\nu;\mu} = 0$ we get that $\rho = \rho_0 a^{-3(1+w)}$. As a result, trace T is in the form

$$T = \sum_i \rho_{i,0}(3w_i - 1)a(t)^{-3(1+w_i)}. \tag{7}$$

In the above equation, parameters w_i correspond to different fluids described by the equation of state $p_i = w_i\rho_i$. We assume baryonic and dark matter ρ_{m} in the form of dust $w = 0$ and dark energy $\rho_\Lambda = \Lambda$ with $w = -1$.

A form of the function $f(\hat{R})$ is unknown. In this paper we assume that the polynomial form of the $f(\hat{R})$ function is in the form

$$f(\hat{R}) = \hat{R} + \gamma\hat{R}^2. \tag{8}$$

The Lagrangian (8) can be treated as a deviation from the lambda cold dark matter (ΛCDM) model by the quadratic Starobinsky term. The Starobinsky model in the Palatini formalism in the cosmological context is considered in [21,43].

A solution of the structural equation (4) has the following form:

$$\hat{R} = -T \equiv 4\Lambda + \rho_{\mathrm{m},0}a^{-3}. \tag{9}$$

Note that solution (9) has the same form in our model as in the ΛCDM model.

The Friedmann equation in our model is given by

$$\frac{H^2}{H_0^2} = \frac{b^2}{(b+\frac{d}{2})^2}\left[\Omega_\gamma(\Omega_{\mathrm{m},0}a^{-3} + \Omega_{\Lambda,0})^2\frac{(K-3)(K+1)}{2b} + (\Omega_{\mathrm{m},0}a^{-3} + \Omega_{\Lambda,0}) + \frac{\Omega_{\mathrm{r},0}a^{-4}}{b} + \Omega_k\right], \tag{10}$$

where $\Omega_k = -\frac{k}{H_0^2a^2}$, $\Omega_{\mathrm{r},0} = \frac{\rho_{\mathrm{r},0}}{3H_0^2}$, $\Omega_{\mathrm{m},0} = \frac{\rho_{\mathrm{m},0}}{3H_0^2}$, $\Omega_{\Lambda,0} = \frac{\Lambda}{3H_0^2}$, $K = \frac{3\Omega_{\Lambda,0}}{(\Omega_{\mathrm{m},0}a^{-3}+\Omega_{\Lambda,0})}$, $\Omega_\gamma = 3\gamma H_0^2$, $b = f'(\hat{R}) = 1 + 2\Omega_\gamma(\Omega_{\mathrm{m},0}a^{-3} + 4\Omega_{\Lambda,0})$, $d = \frac{1}{H}\frac{db}{dt} = -2\Omega_\gamma(\Omega_{\mathrm{m},0}a^{-3} + \Omega_{\Lambda,0})(3-K)$, H_0 is the present value of Hubble function, $\rho_{\mathrm{r},0}$ is the present value of the energy density of radiation and $\rho_{\mathrm{m},0}$ is the present value of the density of matter. For simplicity, henceforth, we consider the model without radiation ($\rho_{\mathrm{r},0} = 0$). Note that for $\gamma = 0$, we get the ΛCDM model.

III. TYPES OF SINGULARITIES IN COSMOLOGY IN THE PALATINI FORMALISM IN THE JORDAN FRAME

In our model, new types of singularities appear which are not contained in the classification of Nojiri *et al.* They are nonisolated singularities. Our model with such singularities is an example of a piecewise smooth dynamical system of the cosmological origin.

Recently, a physically relevant solution of general relativity of the typical black hole spacetimes which admit C^0-metric extensions beyond the future Cauchy horizon has focused mathematicians' attention [59] because this discovery is related to the fundamental issues concerning the strong cosmic censorship conjecture. In his paper, Sbierski [59] noted that the Schwarzschild solution in the global Kruskal-Szekeres coordinates is C^0-extendible.

Galloway and Ling [60] reviewed some aspects of Sbierski's methodology in the general relativity context of cosmological solutions, and use similar techniques to Sbierski in the investigation of the C^0 extendibility of open Friedmann-Lemaître-Robertson-Walker (FLRW) cosmological models. They found that a certain special class of open FLRW spacetimes, which we have dubbed "Milne-like," actually admits the C^0 extension through the big bang. [60–62].

Sbierski has presented recently a new version of his original proof of the C^0 inextendibility of the maximal analytic Schwarzschild spacetime [63]. He deviates from his original proof by using the result, established in collaboration with Galloway and Ling [63], that given the C^0 extension of a globally hyperbolic spacetime, one can find a timelike geodesic that leaves this spacetime. Consequently, this result simplifies greatly the Sbierski proof of the inextendibility through the exterior region of the Schwarzschild spacetime.

The above-mentioned fact and phase portraits suggest that models with the sewn type of singularity can belong to a new class of metrics which admits C^0 extension like in the Milne-like model.

In our model, we find two new types of singularities, which are a consequence of the Palatini formalism: the sewn freeze and sewn sudden singularity. Generally, the freeze singularity takes place when the scale factor a is finite and H, ρ and p are blown up [49] or divergent [52], and the sudden singularity is when the scale factor a, ρ and H are finite and $\dot{H}$ and p are divergent [45]. The freeze

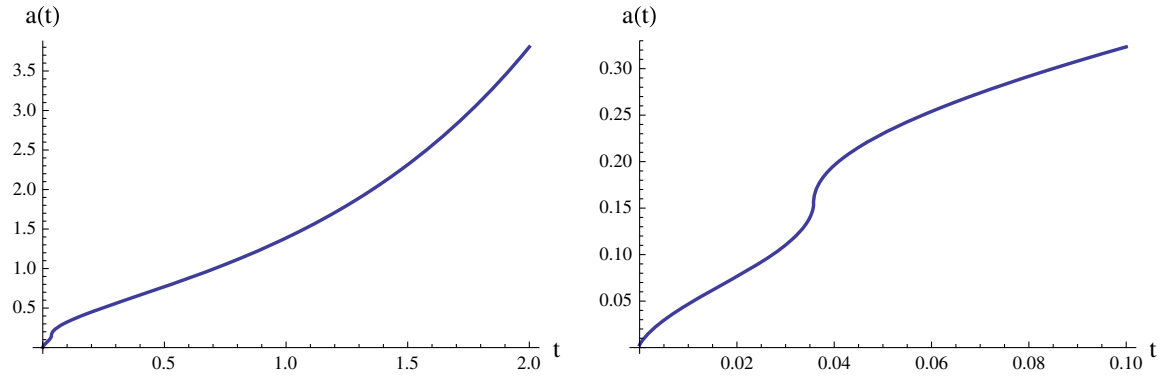

FIG. 1. The left panel presents the illustration of the evolution of the scale factor of the model (10) for the positive parameter γ for the flat universe. The right panel presents a close-up of the left panel in the neighborhood of the sewn freeze singularity (at the vertical inflection point). The value of the parameter γ is chosen as 10^{-6} $\frac{\mathrm{s}^2\,\mathrm{Mpc}^2}{\mathrm{km}^2}$. The cosmological time is expressed in $\frac{\mathrm{s\,Mpc}}{100\ \mathrm{km}}$.

singularity appears when the expression $\frac{b}{b+d/2}$, in the Friedmann equation (10), is equal to infinity. The evolution of the scale factor of the model (10) through the sewn freeze singularity is presented in Fig. 1. The sewn sudden singularity appears when $\frac{b}{b+d/2}$ is equal to zero. This condition is equivalent to $b=0$. The evolution of the scale factor of the model (10) through the sewn sudden singularity is presented in Fig. 2.

When the parameter γ is positive, the sewn freeze singularity appears. In this case, the evolution of the universe in our model and ΛCDM model are equivalent, except the freeze singularity. The evolution starts from the big bang and follows by the deceleration phase. Then the acceleration phase appears in the neighborhood of the sewn freeze singularity. In this singularity, the Hubble function

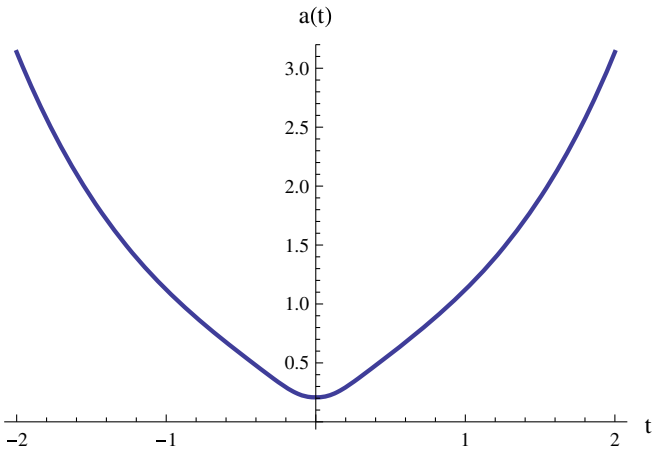

FIG. 2. The illustration of the evolution of the scale factor of the model (10) through the sewn sudden singularity (at the inflection point) for the flat universe. The model with the negative parameter Ω_γ has a mirror symmetry with respect to the cosmological time t. The bounce is at $t=0$. The value of parameter γ is chosen as -10^{-6} $\frac{\mathrm{s}^2\,\mathrm{Mpc}^2}{\mathrm{km}^2}$. The cosmological time is expressed in $\frac{\mathrm{s\,Mpc}}{100\ \mathrm{km}}$.

reaches the infinity value, which corresponds to the pole of the potential function. In this time, the inflation appears. After the inflation phase, the universe decelerates and the evolution is similar to the evolution in the ΛCDM model. The main physical effect of the sewn freeze singularity is the inflation, but its influence on the evolution of the universe is minor because the number of e-folds is too small [64].

In the case of the negative parameter γ, the big bang does not appear because it is replaced by the bounce, which corresponds with the sewn sudden singularity. In this singularity, the value of the Hubble function is zero. When the bounce is reached, the acceleration and next the deceleration phase appears. Afterwards, the behavior of the universe is like that in the ΛCDM model.

After an explicit application of geodesic equation to the Friedmann cosmology, one can find out whether geodesics can be prolonged through a singularity, i.e., about the geodesic incompleteness of the spacetime. Let us note that geodesics do not feel a singularity at all—they are not singular there since, for example $a_\mathrm{s}=a(t_\mathrm{s})=\mathrm{const}$ at $t=t_\mathrm{s}$ being the time of a singularity, and there is no geodesic incompleteness [65].

A deeper insight in the structure of singularities can be obtained from the geodesic deviation equation (which measures the behavior of a bunch of geodesics). It is important that this equation does feel singularities since at $t=t_\mathrm{s}$ the Riemann tensor $R_{\alpha\beta\mu\nu}\to\infty$. As an example we see that with the sudden singularity it is possible to "go through" the singularity since we have

$$R^{\alpha}{}_{0\beta0}=-\frac{\ddot{a}}{a}\delta^{\alpha}{}_{\beta},\ (\dot{\ldots})=\frac{\partial}{\partial t}, \tag{11}$$

$$\dot{u}^{\alpha}=-R^{\alpha}{}_{0\beta0}n^{\beta}\propto\ddot{a}\propto-\frac{\partial V}{\partial a}, \tag{12}$$

where $\delta^{\alpha}{}_{\beta}$ is the Kronecker delta, u^{α} is the four-velocity vector and n^{α} is the deviation vector separating neighboring

geodesics (particle worldlines) which describes the propagation of the distance between geodesics.

The curvature tensor feels, for example, the sudden singularity because the Riemann tensor diverges to minus infinity at $t = t_s$.

Physically, it means that the tidal forces which manifest here as the (infinite) impulse which reverses (or stops) the increase of separation of geodesics and the geodesics themselves can evolve further—the universe can continue its evolution through a singularity.

In our model, the sewn freeze singularity is a solution of the following algebraic equation:

$$2b + d = 0 \tag{13}$$

or

$$-3K - \frac{K}{3\Omega_\gamma(\Omega_m + \Omega_{\Lambda,0})\Omega_{\Lambda,0}} + 1 = 0, \tag{14}$$

where $K \in [0, 3)$.

The solution of Eq. (14) is

$$K_{\text{freeze}} = \frac{1}{3 + \frac{1}{3\Omega_\gamma(\Omega_m+\Omega_{\Lambda,0})\Omega_{\Lambda,0}}}. \tag{15}$$

We obtain an expression for a value of the scale factor at the freeze singularity from Eq. (15),

$$a_{\text{freeze}} = \left(\frac{1-\Omega_{\Lambda,0}}{8\Omega_{\Lambda,0} + \frac{1}{\Omega_\gamma(\Omega_m+\Omega_{\Lambda,0})}}\right)^{\frac{1}{3}}. \tag{16}$$

We get the sewn sudden singularity when $b = 0$. This gets us the following algebraic equation:

$$1 + 2\Omega_\gamma(\Omega_{m,0}a^{-3} + 4\Omega_{\Lambda,0}) = 0. \tag{17}$$

From Eq. (17), we get the formula for the scale factor at a sewn sudden singularity,

$$a_{\text{sudden}} = \left(-\frac{2\Omega_{m,0}}{\frac{1}{\Omega_\gamma} + 8\Omega_{\Lambda,0}}\right)^{1/3}. \tag{18}$$

We can rewrite Eq. (10) as a dynamical system. We choose a and $y = a'$, where $' \equiv \frac{d}{d\sigma} = \frac{b+\frac{d}{2}}{b}\frac{d}{dH_0 t}$ is a new parametrization of time, as the variables of the dynamical system. We derive these variables with respect to the σ time using Eq. (10) and we get the following equations of the dynamical system:

$$a' = y, \tag{19}$$

$$y' = -\frac{\partial V(a)}{\partial a}, \tag{20}$$

where

$$V = -\frac{a^2}{2}\left[\Omega_\gamma(\Omega_{m,0}a^{-3} + 4\Omega_{\Lambda,0})^2\frac{(K-3)(K+1)}{2b} + (\Omega_{m,0}a^{-3} + 4\Omega_{\Lambda,0})\right]. \tag{21}$$

We can treat the dynamical system [(19)–(20)] as a sewn dynamical system [66,67]. In this case, the phase portrait is divided into two regions: the first part is for $a < a_{\text{sing}}$ and the second part is for $a > a_{\text{sing}}$. Both parts are sewn along the singularity.

For $a < a_{\text{sing}}$, we can rewrite the dynamical system [(19)–(20)] in the corresponding form

$$a' = y, \tag{22}$$

$$y' = -\frac{\partial V_1(a)}{\partial a}, \tag{23}$$

where $V_1 = V(-\eta(a - a_s) + 1)$ and $\eta(a)$ denotes the Heaviside function.

For $a > a_{\text{sing}}$, we get in an analogous way the following equations:

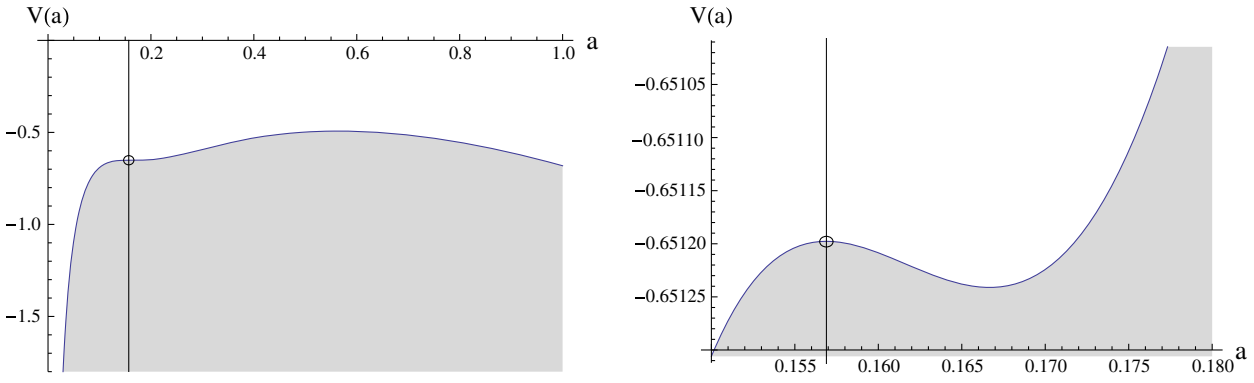

FIG. 3. The left panel presents the diagram of the potential $V(a)$ (21) for the positive parameter γ. The right panel presents a close-up of the left diagram in the neighborhood of the sewn singularity. The vertical line represents the sewn freeze singularity. The parameter γ is chosen as $10^{-6}\ \frac{s^2\,\text{Mpc}^2}{\text{km}^2}$. Note that for $a = a_{\text{sing}}$, $V(a)$ is undefined.

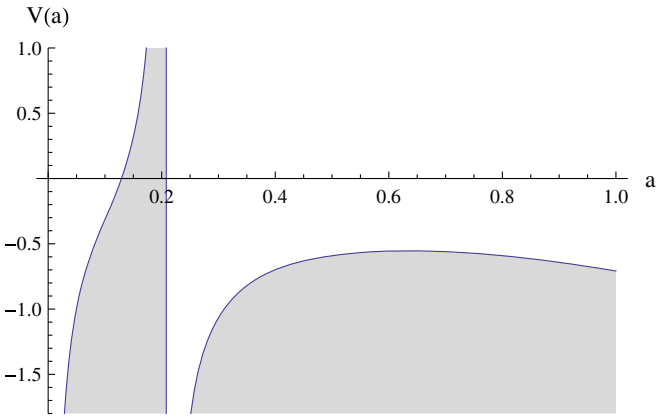

FIG. 4. The diagram of the potential $V(a)$ (21) for the negative parameter γ. The vertical line represents the sewn sudden singularity. The parameter γ is chosen as $-10^{-6}\,\frac{s^2\,\mathrm{Mpc}^2}{\mathrm{km}^2}$.

$$a' = y, \tag{24}$$

$$y' = -\frac{\partial V_2(a)}{\partial a}, \tag{25}$$

where $V_2 = V\eta(a - a_s)$.

The diagrams of the potential function $V(a)$ (21) are presented in Fig. 3 for the positive parameter γ and in Fig. 4 for the negative parameter γ. The phase portraits of the system can be constructed similarly as in classical mechanics due to the particlelike description of dynamics. Phase trajectories representing evolutionary paths can be obtained directly from the geometry of potential function $V(a)$ by consideration of constant energy levels $(a')^2/2 + V(a) = E = \mathrm{const} = -k/2$. The reparametrized time parameter σ is measured along the trajectories of the corresponding dynamical system. It has a sense of a diffeomorphic transformation beyond the singularity vertical line.

The potential function (21) is undefined at the singularity point $a = a_{\mathrm{sing}}$. Therefore, in phase portraits of the system in the Jordan frame, there are two domains separated by a line of singularity points. These phase portraits are constructed by the application of the diffeomorphic reparametrization of cosmological time beyond this singularity line and then C^1 sewing of trajectories. As a result, we obtain that only one unique trajectory moves at any point in the phase space.

The phase portraits for the system [(19)–(20)] for positive Ω_γ are presented in Fig. 5 and for negative Ω_γ in Fig. 6. The line of singularity points is represented by a dashed line.

We find that the system [(19)–(20)] for positive Ω_γ has a sequence of three critical points located on the a axis (saddle-center-saddle sequence). To clarify the behavior of trajectories in the neighborhood of the saddle located at the singularity line we present a close-up of this area in Fig. 5 (see the right panel).

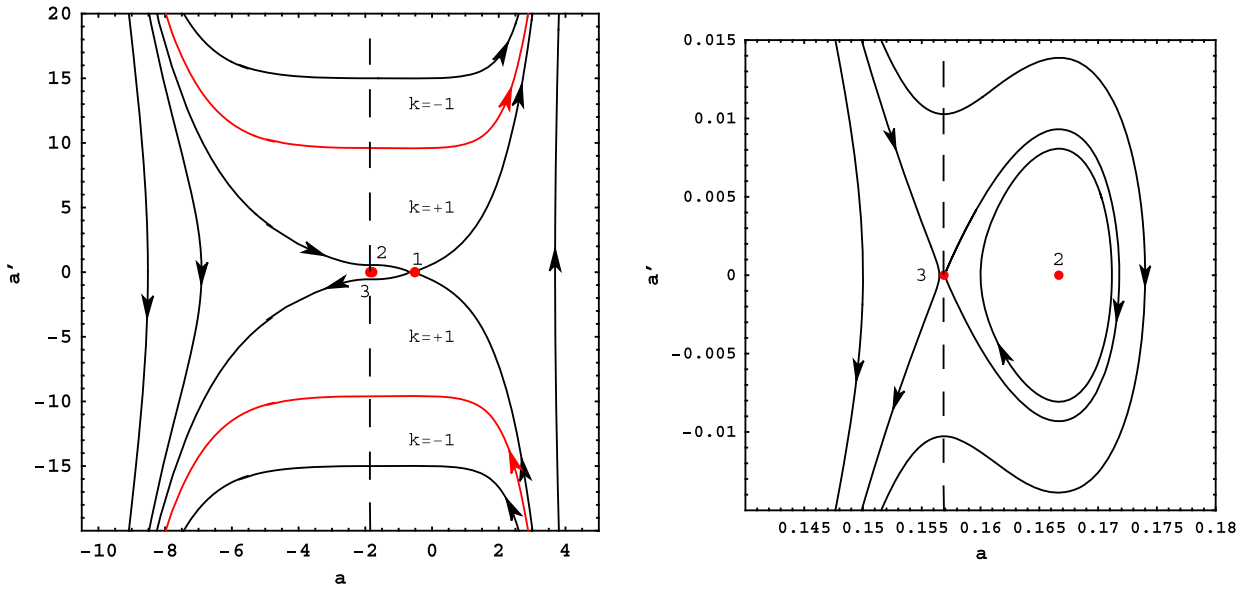

FIG. 5. The left panel is the phase portrait of the system [(19)–(20)] with the positive parameter Ω_γ. The right panel is a close-up of the left panel in the neighborhood of critical points 2 and 3. The value of parameter γ is chosen as $10^{-6}\,\frac{s^2\,\mathrm{Mpc}^2}{\mathrm{km}^2}$. The value of $\Omega_{\Lambda,0}$ is chosen as 0.7 and the present value of the Hubble function is chosen as $68\,\frac{\mathrm{km}}{\mathrm{s\,Mpc}}$. The scale factor a is presented in the natural logarithmic scale. The spatially flat universe is represented by the red trajectories. The dashed line $2b + d = 0$ represents the freeze singularity. The critical points 1, 2 and 3 represent the static Einstein universes. The phase portrait belongs to the class of sewn dynamical systems. Note that the existence of the homoclinic orbit which starts at $t = -\infty$ and approach at $t = +\infty$. In the interior of this orbit, there are located trajectories representing oscillating cosmological models. They are free from initial and final singularities.

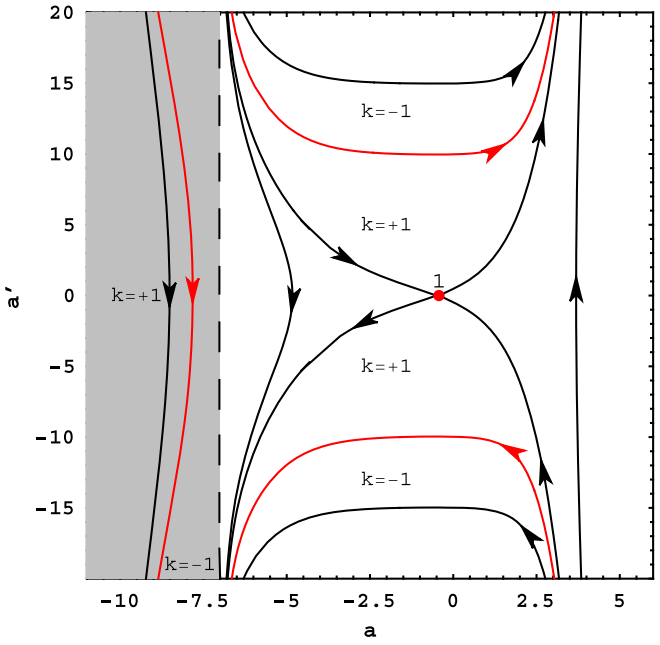

FIG. 6. The phase portrait of the system [(19)–(20)] with the negative parameter Ω_γ. The value of the parameter γ is chosen as $-10^{-13}\,\frac{\mathrm{s}^2\,\mathrm{Mpc}^2}{\mathrm{km}^2}$. The value of $\Omega_{\Lambda,0}$ is chosen as 0.7 and the present value of the Hubble function is chosen as $68\,\frac{\mathrm{km}}{\mathrm{s\,Mpc}}$. The scale factor a is presented in the natural logarithmic scale. The spatially flat universe is represented by the red trajectories. The dashed line separates the domain where $a < a_{\mathrm{sing}}$ from the domain where $a > a_{\mathrm{sing}}$. The shaded region represents trajectories with $b < 0$. If we assume that $f'(R) > 0$, then this region can be removed. Critical point 1 represents the static Einstein universe. The critical points at infinity, $a = a_{\mathrm{sing}}$, $a' = \pm\infty$ represent typical sudden singularities. The phase portrait belongs to the class of sewn dynamical systems.

In Fig. 6 the critical points at infinity, $a = a_{\mathrm{sing}}, a' = \pm\infty$ represent typical sudden singularities. There are two types of sewn trajectories: one homoclinic orbit and infinity of periodic orbits. The homoclinic orbit starts from the neighborhood of critical point 1, goes to the singularity at $a' = -\infty$ and, after sewing with the trajectory which comes from the singularity at $a' = +\infty$, finishes at the saddle point 1. The periodic orbits are situated inside the domain bounded by the homoclinic orbit. Similarly to the homoclinic orbit, the periodic orbits are sewn when going to the minus infinity singularity and going out from the plus infinity singularity. Note that these periodic orbits are possible only in the $k = +1$ universe. There are also nonperiodic trajectories which lie inside the two regions bounded by the separatrices of the saddle 1. The trajectories start at $a' = -\infty$, approach saddle 1, go to the minus infinity singularity after sewing go out from the plus infinity singularity, approach saddle 1 and then continue to $a' = +\infty$. This kind of evolution is possible for the flat universe as well as $k = -1$ and $k = +1$ universes. Finally, in the region on the right of the separatrices of saddle 1, the trajectories start at $a' = -\infty$ and go to $a' = +\infty$, representing the evolution without a sewn sudden singularity of the $k = +1$ universes.

The critical points of the dynamical system [(19)–(20)] are completed in Table I.

The action (1) can be rewritten as

$$S = S_{\mathrm{g}} + S_{\mathrm{m}} = \frac{1}{2}\int \sqrt{-g}\phi\hat{R}d^4x + S_{\mathrm{m}}, \tag{26}$$

where $\phi = \frac{f(\hat{R})}{\hat{R}}$. Let G_{eff} mean the effective gravitational constant. Then $\phi = \frac{1}{8\pi G_{\mathrm{eff}}}$ and in the consequence $G_{\mathrm{eff}}(\hat{R}) = \frac{\hat{R}}{8\pi f(\hat{R})}$ and especially for $f(\hat{R}) = \hat{R} + \gamma\hat{R}^2$ has the following form:

$$\frac{G_{\mathrm{eff}}(\hat{R})}{G} = \frac{1}{1+\gamma\hat{R}}. \tag{27}$$

The evolution of G_{eff} is presented in Fig. 7. Note that the value of G_{eff} for $t = 0$ is equal to zero and approaches asymptotically to the value of gravitational constant.

IV. THE PALATINI FORMALISM IN THE EINSTEIN FRAME

Scalar-tensor theories of gravity can be formulated in the Jordan and in the Einstein frames. These frames are conformally related [68]. We know that the formulations of a scalar-tensor theory in two different conformal frames are physically inequivalent. There was a remarkable progress in the understanding of the geometric features of the Palatini theories and the role of the choice of a frame in the last years [69,70]. Considering the model in the

TABLE I. Critical points of the dynamical system [(19)–(20)]. They are also presented in Fig. 5. All three critical points represent a static Einstein universe.

No. of critical point	Coordinates of critical point	Type of critical point
1	$\left(a = \left(\frac{8\gamma\Lambda^2-\Lambda+3H_0^2(1-8\gamma\Lambda)+(3H_0^2-\Lambda)\sqrt{(1-24\gamma\Lambda)}}{4\Lambda(1+8\gamma\Lambda)}\right)^{1/3}, a' = 0\right)$	saddle
2	$\left(a = \left(\frac{8\gamma\Lambda^2-\Lambda+3H_0^2(1-8\gamma\Lambda)-(3H_0^2-\Lambda)\sqrt{(1-24\gamma\Lambda)}}{4\Lambda(1+8\gamma\Lambda)}\right)^{1/3}, a' = 0\right)$	center
3	$\left(a = \frac{(\gamma(3H_0^2-\Lambda))^{1/3}}{(1+8\gamma\Lambda)^{1/3}}, a' = 0\right)$	saddle

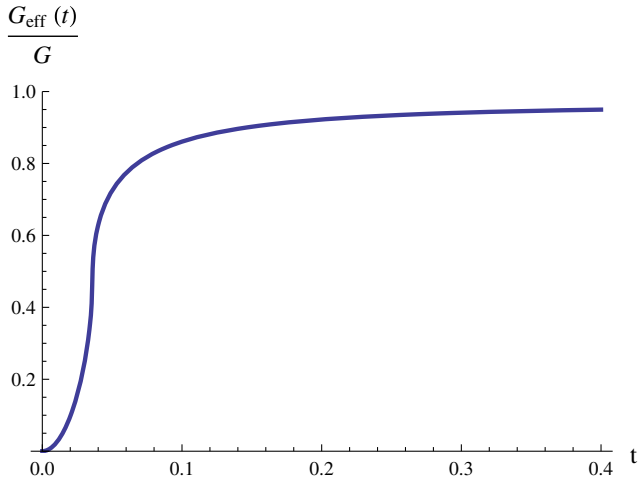

FIG. 7. The evolution of $G_{\rm eff}$ for the positive parameter γ and the flat universe. The cosmological time t is expressed in $\frac{\rm s\,Mpc}{100\ \rm km}$. The parameter γ is chosen as $10^{-6}\,\frac{\rm s^2\,Mpc^2}{\rm km^2}$. Note that when $t\to\infty$ then $\frac{G_{\rm eff}(t)}{G}\to\frac{1}{1+4\gamma\Lambda}$.

Einstein frame in the Palatini formalism, we find that the big bang singularity is replaced by the singularity of the finite scale factor and that some pathologies, like degenerated multiple freeze singularities [64], disappear in a generic case.

If $f''(\hat{R})\neq 0$, then action (1) is dynamically equivalent to the first order Palatini gravitational action [1,12,36]

$$S(g_{\mu\nu},\Gamma^{\lambda}_{\rho\sigma},\chi) =\frac{1}{2}\int {\rm d}^4x\sqrt{-g}(f'(\chi)(\hat{R}-\chi)+f(\chi))+S_m(g_{\mu\nu},\psi). \quad (28)$$

Let $\Phi=f'(\chi)$ be a scalar field and $\chi=\hat{R}$. Then action (28) can be rewritten in the following form:

$$S(g_{\mu\nu},\Gamma^{\lambda}_{\rho\sigma},\Phi)=\frac{1}{2}\int {\rm d}^4x\sqrt{-g}(\Phi\hat{R}-U(\Phi))+S_m(g_{\mu\nu},\psi), \quad (29)$$

where the potential $U(\Phi)$ is defined by

$$U_f(\Phi)\equiv U(\Phi)=\chi(\Phi)\Phi-f(\chi(\Phi)), \quad (30)$$

where $\Phi=\frac{df(\chi)}{d\chi}$ and $\hat{R}\equiv\chi=\frac{dU(\Phi)}{d\Phi}$.

We can get from the Palatini variation of the action (29) the following equations of motion:

$$\Phi\left(\hat{R}_{\mu\nu}-\frac{1}{2}g_{\mu\nu}\hat{R}\right)+\frac{1}{2}g_{\mu\nu}U(\Phi)-T_{\mu\nu}=0, \quad (31a)$$

$$\hat{\nabla}_{\lambda}(\sqrt{-g}\Phi g^{\mu\nu})=0, \quad (31b)$$

$$\hat{R}-U'(\Phi)=0. \quad (31c)$$

From Eq. (31b), we get that the connection $\hat{\Gamma}$ is a metric connection for a new metric $\bar{g}_{\mu\nu}=\Phi g_{\mu\nu}$; thus, $\hat{R}_{\mu\nu}=\bar{R}_{\mu\nu}$, $\bar{R}=\bar{g}^{\mu\nu}\bar{R}_{\mu\nu}=\Phi^{-1}\hat{R}$ and $\bar{g}_{\mu\nu}\bar{R}=g_{\mu\nu}\hat{R}$. The g trace of (31a) gives a new structural equation,

$$2U(\Phi)-U'(\Phi)\Phi=T. \quad (32)$$

The question of whether the metric $g_{\mu\nu}$ or $\bar{g}_{\mu\nu}$ has the physical meaning is a problem of the interpretation of these functions. It is strictly related to the problem of a choice of the frame (Einstein frame or Jordan frame). Some people claim that a conformally rescaled metric by a scalar field is only an mathematical trick without a physical meaning. However, the objectivity of investigation requires the consideration of both cases. In our opinion, only astronomical observations can resolve this question [71]. In this section, we also consider that $\bar{g}_{\mu\nu}$ has the physical meaning in the Einstein frame. We are looking for such a choice of the frame in which inflation can be reproduced in analogy to the Starobinsky model. Unfortunately, it is not the case of the Jordan case. Azri [72] tried to answer the question about the reality of conformal frames in the context of the nonminimal coupling dynamics of a single scalar field in purely affine gravity. In this approach, the coupling is performed via an affine connection and its associated curvature without referring to any metric tensor. It is interesting that in affine gravity the transition from nonminimal to minimal couplings is realized by only field redefinition of the scalar field. As a result, the inflationary models gain a unique description in this context where observed parameters are invariant under a field reparametrization. The inflation in the Starobinsky model is realized in the Einstein frame but it would be nice to find the realization of the inflation as a phenomenon which is invariant under the redefinition of the scalar field.

Now Eqs. (31a) and (31c) take the following forms:

$$\bar{R}_{\mu\nu}-\frac{1}{2}\bar{g}_{\mu\nu}\bar{R}=\bar{T}_{\mu\nu}-\frac{1}{2}\bar{g}_{\mu\nu}\bar{U}(\Phi), \quad (33)$$

$$\Phi\bar{R}-(\Phi^2\bar{U}(\Phi))'=0, \quad (34)$$

where $\bar{U}(\phi)=U(\phi)/\Phi^2$, $\bar{T}_{\mu\nu}=\Phi^{-1}T_{\mu\nu}$ and the structural equation can be replaced by

$$\Phi\bar{U}'(\Phi)+\bar{T}=0. \quad (35)$$

As a result, the action for the metric $\bar{g}_{\mu\nu}$ and scalar field Φ is given in the following form:

$$S(\bar{g}_{\mu\nu},\Phi)=\frac{1}{2}\int {\rm d}^4x\sqrt{-\bar{g}}(\bar{R}-\bar{U}(\Phi))+S_m(\Phi^{-1}\bar{g}_{\mu\nu},\psi), \quad (36)$$

where a nonminimal coupling is between Φ and $\bar{g}_{\mu\nu}$,

$$\bar{T}^{\mu\nu}=-\frac{2}{\sqrt{-\bar{g}}}\frac{\delta}{\delta\bar{g}_{\mu\nu}}S_m=(\bar{\rho}+\bar{p})\bar{u}^{\mu}\bar{u}^{\nu}+\bar{p}\bar{g}^{\mu\nu}=\Phi^{-3}T^{\mu\nu}, \quad (37)$$

$\bar{u}^\mu = \Phi^{-\frac{1}{2}} u^\mu$, $\bar{\rho} = \Phi^{-2}\rho, \bar{p} = \Phi^{-2}p$, $\bar{T}_{\mu\nu} = \Phi^{-1}T_{\mu\nu}, \bar{T} = \Phi^{-2}T$ [12,73].

In the FRW metric case, metric $\bar{g}_{\mu\nu}$ has the following form:

$$d\bar{s}^2 = -d\bar{t}^2 + \bar{a}^2(\bar{t})[dr^2 + r^2(d\theta^2 + \sin^2\theta d\phi^2)], \quad (38)$$

where $d\bar{t} = \Phi(t)^{\frac{1}{2}}dt$ and new scale factor $\bar{a}(\bar{t}) = \Phi(\bar{t})^{\frac{1}{2}}a(\bar{t})$. Because we assume the barotropic matter, the cosmological equations are given by

$$3\bar{H}^2 = \bar{\rho}_\Phi + \bar{\rho}_m, \qquad 6\frac{\ddot{\bar{a}}}{\bar{a}} = 2\bar{\rho}_\Phi - \bar{\rho}_m(1+3w), \quad (39)$$

where

$$\bar{\rho}_\Phi = \frac{1}{2}\bar{U}(\Phi), \qquad \bar{\rho}_m = \rho_0 \bar{a}^{-3(1+w)}\Phi^{\frac{1}{2}(3w-1)} \quad (40)$$

and $w = \bar{p}_m/\bar{\rho}_m = p_m/\rho_m$. The conservation equation gets the following form:

$$\dot{\bar{\rho}}_m + 3\bar{H}\bar{\rho}_m(1+w) = -\dot{\bar{\rho}}_\Phi. \quad (41)$$

In the case of the Starobinsky-Palatini model, the potential $\bar{U}$ is described by the following formula:

$$\bar{U}(\Phi) = 2\bar{\rho}_\Phi(\Phi) = \left(\frac{1}{4\gamma} + 2\lambda\right)\frac{1}{\Phi^2} - \frac{1}{2\gamma}\frac{1}{\Phi} + \frac{1}{4\gamma}. \quad (42)$$

V. A COMPARISON OF THE JORDAN FRAME AND THE EINSTEIN FRAME IN THE PALATINI FORMALISM

If we consider dynamics in the Jordan frame, then one can use a formula for H^2 to reduce the dynamics to the dynamical system of the Newtonian type which possesses the first integral $\frac{1}{2}(\frac{da}{dt})^2 + V(a) = 0$, where $V(a) = -\frac{1}{2}H^2a^2$. In this representation of dynamics, singularities for the finite value of the scale factor $a = a_s$ are poles of $V(a)$ potential or their derivatives. Stachowski *et al.* [64] investigated these type of singularities in detail. The generic feature of the formulation of dynamics is the appearance of the freeze or typical sudden type of singularity in the past. At the freeze singularity point while the scale factor is finite, its second derivative with respect to the time blows up, i.e., $\frac{d^2a}{dt^2} = \pm\infty$. In general, all singularities can be detected from the diagram of the potential function.

If we consider dynamics in the Einstein frame, there are no such singularities. The big bang singularity present in the ΛCDM model is replaced by the generalized sudden singularity of the finite scale factor. Beyond this singularity, the phase portrait is equivalent to the ΛCDM model.

Two dynamical systems in the phase space are equivalent if there is a homeomorphism transforming all trajectories with the preserving of the direction of time measured along the trajectories. The comparison of dynamics in both the Jordan and Einstein frames explicitly shows that corresponding dynamical systems are not topologically equivalent. Consequently, the physics in both frames is different.

The cosmological equation for the Starobinsky-Palatini model in the Einstein frame can be rewritten to the form of the dynamical system with the Hubble parameter $\bar{H}(\bar{t})$ and the Ricci scalar $\hat{R}(\bar{t})$ as variables,

$$\dot{\bar{H}}(\bar{t}) = \frac{1}{6(1+2\gamma\hat{R}(\bar{t}))^2}(6\Lambda - 6\bar{H}(\bar{t})^2(1+2\gamma\hat{R}(\bar{t}))^2 + \hat{R}(\bar{t})(-1+24\gamma\Lambda+\gamma(1+24\gamma\Lambda)\hat{R}(\bar{t}))), \quad (43)$$

$$\dot{\hat{R}}(\bar{t}) = -\frac{3}{(-1+\gamma\hat{R}(\bar{t}))}\bar{H}(\bar{t})(1+2\gamma\hat{R}(\bar{t}))(4\Lambda+\hat{R}(\bar{t}) \times(-1+16\gamma\Lambda+16\gamma^2\Lambda\hat{R}(\bar{t}))), \quad (44)$$

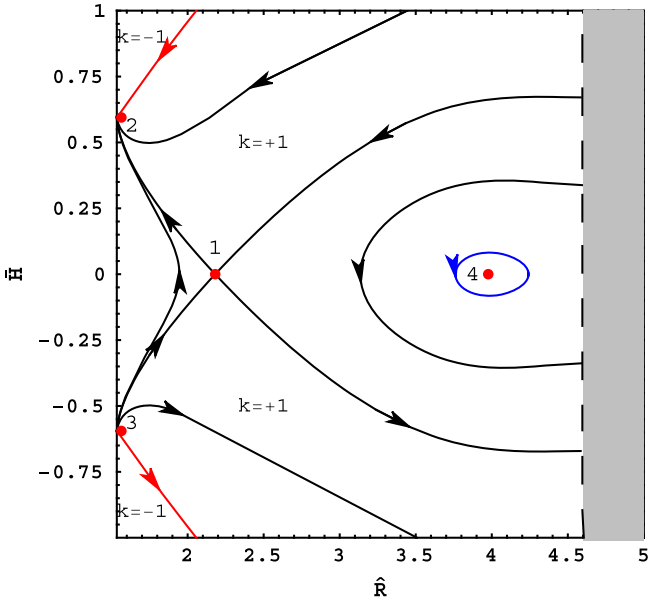

FIG. 8. The phase portrait of system (43)–(44). There are four critical points: point 1 represents the Einstein universe, point 2 represents the stable de Sitter universe, point 3 represents the unstable de Sitter universe and point 4 represents the Einstein universe. The value of the parameter γ is chosen as $10^{-6}\frac{s^2\,Mpc^2}{km^2}$. The value of $\Omega_{\Lambda,0}$ is chosen as 0.7 and the present value of the Hubble function is chosen as $68\frac{km}{s\,Mpc}$. The values of the Hubble function are given in $\frac{100\ km}{s\,Mpc}$ and the values of the Ricci scalar are given in $\frac{10^4\ km^2}{s^2\ Mpc^2}$ in the natural logarithmic scale. The gray color represents the nonphysical domain. The dashed line represents the generalized sudden singularity. Note that for the Starobinsky-Palatini model in the Einstein frame for the positive parameter γ, the sewn freeze singularity is replaced by the generalized sudden singularity. A typical trajectory in the neighborhood of the trajectory of the flat model (represented by the red trajectory) starts from the generalized sudden singularity then goes to the de Sitter attractor. The position of this attractor is determined by the cosmological constant parameter. Oscillating models (blue trajectory) are situated around critical point 4.

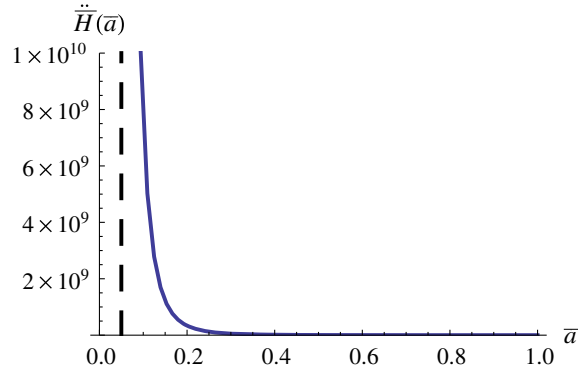

FIG. 9. The relation $\ddot{H}(\bar{a})$ for the Palatini formalism in the Einstein frame. The value of the parameter γ is chosen as $10^{-9}\ \frac{\mathrm{s^2\,Mpc^2}}{\mathrm{km^2}}$. The values of the $\ddot{H}(\bar{a})$ are given in $\frac{\mathrm{km^3}}{\mathrm{s^3\,Mpc^3}}$. The dashed line represents the generalized sudden singularity. Note that, in the generalized sudden singularity, H and $\dot{H}$ are finite but $\ddot{H}$ and its derivatives are divergent.

where a dot denotes the differentiation with respect to the time $\bar{t}$. The phase portrait for the dynamical system [(43)–(44)] is presented in Fig. 8. Here, the periodic orbits appear around critical point 4. In the Starobinsky-Palatini model in the Einstein frame appears the generalized sudden singularity, for which H and $\dot{H}$ are finite but $\ddot{H}$ and its derivatives are diverge (see Fig. 9). The evolution of the scale factor begins from a finite value different from zero (see Fig. 10). In terms of the scale factor, at the singularity for the finite value of the scale factor $\bar{a}$, a third time derivative (and higher orders) of the scale factor in Einstein frame blows up, while first and second order time derivatives behave regularly. The evolution of the scale factor for one of these periodic orbits is presented in Fig. 11. When matter is negligible, then the inflation appears. In this case, $a \approx a_0 \exp\left(\frac{t}{4}\sqrt{\frac{1+\sqrt{1-32\gamma\Lambda}}{3\gamma}}\right)$, where $a_0 = a(0)$ and $R(t) \approx \frac{1-16\gamma\Lambda+\sqrt{1-32\gamma\Lambda}}{32\gamma^2\Lambda}$ [74]. If $\gamma > \frac{1}{36\Lambda}$, then the nonphysical domain appears for $\hat{R} < \frac{1-16\gamma\Lambda+\sqrt{1-32\gamma\Lambda}}{32\gamma^2\Lambda}$ for which $\rho_{\mathrm{m}} < 0$.

For comparison of the dynamical systems in both frames, we obtain the dynamical system for the Starobinsky-Palatini model in the Jordan frame in the variables $H(t)$ and $\hat{R}(t)$

$$\dot{H}(t) = -\frac{1}{6}\left[6(2\Lambda + H(t)^2) + \hat{R}(t) + \frac{18(1+8\gamma\Lambda)(\Lambda - H(t)^2)}{-1-12\gamma\Lambda+\gamma\hat{R}(t)} - \frac{18(1+8\gamma\Lambda)H(t)^2}{1+2\gamma\hat{R}(t)}\right], \tag{45}$$

$$\dot{\hat{R}}(t) = -3H(t)(\hat{R}(t) - 4\Lambda), \tag{46}$$

where a dot means the differentiation with respect to time t. The phase portrait for the dynamical system (45)–(46) is shown in Fig. 12 (see left panel). This phase portrait represents all evolutionary paths of the system in the Jordan frame without adopting the time reparametrization. Along the trajectories is measured the original cosmological time t. The system [(45)–(46)] constitutes a two-dimensional autonomous dynamical system. Let us note that while the Ricci scalar $\hat{R}$ is related with a second time derivative of the scale factor a, the Hubble function H is related with a first time derivative of the scale factor a. The oscillating orbits appear around critical point 4 (see Fig. 12). The evolution of the scale factor for one of these periodic orbits is presented in Fig. 13.

For a deeper analysis of the behavior of the trajectories of system (45)–(46) in the infinity, we introduce variables $\hat{R}$ and $W = \frac{H}{\sqrt{1+H^2}}$ and rewrite Eqs. (45)–(46) in these variables. Then we get the following dynamical system:

$$\dot{W}(t) = \frac{\dot{H}(t)}{(1+H(t)^2)^{3/2}} = -\frac{(1-W(t)^2)^{3/2}}{6}\left[6\left(2\Lambda + \frac{W(t)^2}{1-W(t)^2}\right) + \hat{R}(t) + \frac{18(1+8\gamma\Lambda)\left(\Lambda - \frac{W(t)^2}{1-W(t)^2}\right)}{-1-12\gamma\Lambda+\gamma\hat{R}(t)} - \frac{18(1+8\gamma\Lambda)\frac{W(t)^2}{1-W(t)^2}}{1+2\gamma\hat{R}(t)}\right], \tag{47}$$

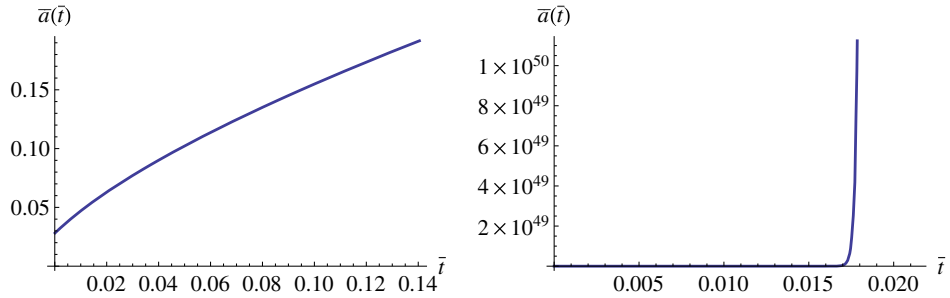

FIG. 10. The illustration of the evolution of the scale factor for the Palatini formalism in the Einstein frame for the flat universe. The left panel presents the case when matter is not negligible. The right panel presents the case when matter is negligible. The value of parameter γ is chosen as $10^{-9}\ \frac{\mathrm{s^2\,Mpc^2}}{\mathrm{km^2}}$. The cosmological time is expressed in $\frac{\mathrm{s\,Mpc}}{\mathrm{km}}$. Note that the evolution of the scale factor begins from a finite value different from zero. Note that when matter is negligible, then the inflation appears (see the right panel). In this case, the number of e-folds is equal to 50.

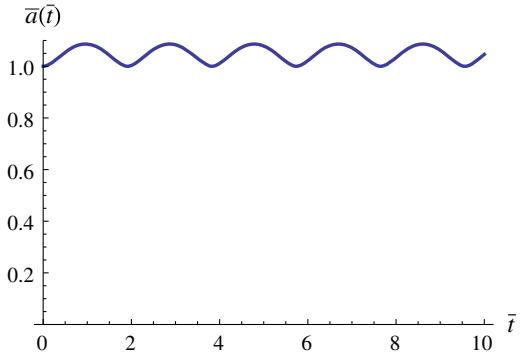

FIG. 11. The diagram presents the evolution of the scale factor for trajectory of the oscillating orbit in the neighborhood of critical point 4 (see Fig. 8). The cosmological time is expressed in $\frac{\text{s Mpc}}{100\ \text{km}}$. Here, $a_{\text{min}} = 1$.

$$\dot{\hat{R}}(t) = -3\frac{W(t)}{\sqrt{1-W(t)^2}}(\hat{R}(t) - 4\Lambda). \tag{48}$$

The phase portrait for dynamical system (47)–(48) is presented in Fig. 12 (the right panel). This portrait is a good illustration of how trajectories are sewn at the points at infinity (points 5 and 6). For expanding models situated on the upper part of the domain, where W is positive, all the trajectories pass through point 6. This continuation of trajectories is the class of C^0. The singularity line represents the freeze type of singularity. There are some differences in the behavior of trajectories of the same model represented in Figs. 5 and 12. While the continuation on the singularity line in Fig. 5 is smooth of C^1 class and the Cauchy problem is correctly solved in Fig. 12, all trajectories from separated regions focused at the degenerated point 6 (and point 5 for contracting models) represent the freeze type of singularity. It has a consequence for the solution of the Cauchy problem. Therefore, the representation of dynamics in the reparametrized time seems to be more suitable than in the original cosmological time.

For the Eqs. (43)–(44) and (45)–(46), we can find the first integrals. In the case of Eqs. (43)–(44), the first integral has the following form:

$$\bar{H}(\bar{t})^2 + \Lambda - \frac{\hat{R}(\bar{t})(2+\gamma\hat{R}(\bar{t}))}{6(1+2\gamma\hat{R}(\bar{t}))^2} + \frac{k}{\bar{a}^2} = 0. \tag{49}$$

Because

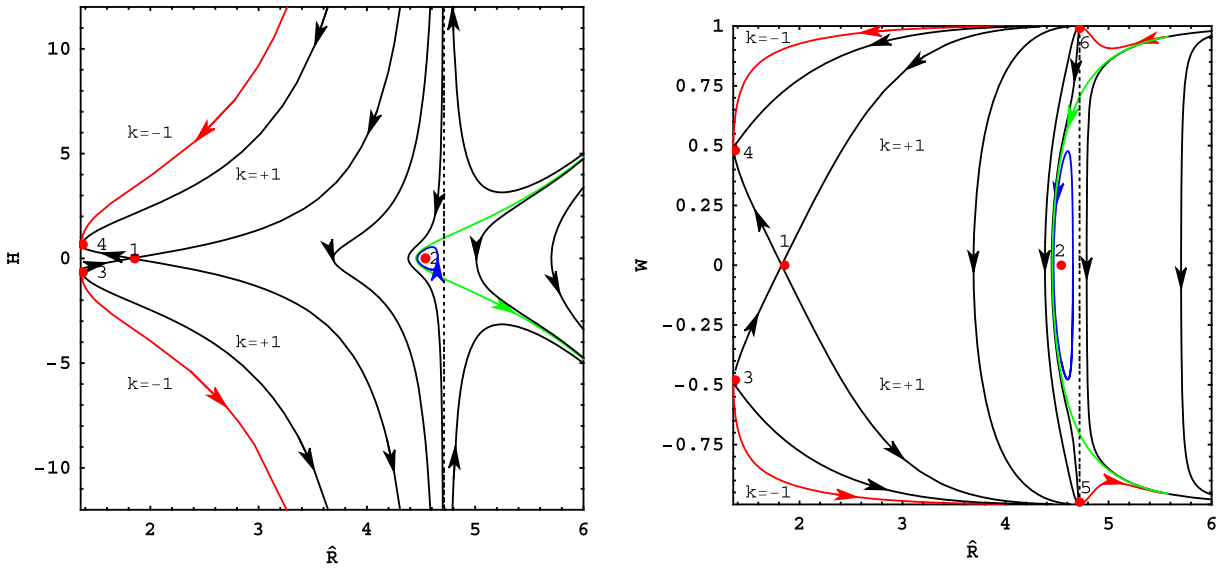

FIG. 12. The left panel is the phase portrait of system (45)–(46) and the right one is the phase portrait of system (47)–(48). There are four critical points in both systems: point 1 and 2 represent the Einstein universe, point 3 represents the unstable de Sitter universe and point 4 represents the stable de Sitter universe. For illustration, the value of the parameter γ is chosen as $10^{-6}\frac{\text{s}^2\,\text{Mpc}^2}{\text{km}^2}$. The value of $\Omega_{\Lambda,0}$ is chosen as 0.7 and the present value of the Hubble function is chosen as $68\frac{\text{km}}{\text{s Mpc}}$. The values of the Hubble function are given in $\frac{100\ \text{km}}{\text{s Mpc}}$ and the values of the Ricci scalar are given in $\frac{10^4\ \text{km}^2}{\text{s}^2\,\text{Mpc}^2}$ in the natural logarithmic scale. The dotted line, representing a line of discontinuity, separates the domain where $\hat{R} < \hat{R}_{\text{sing}} = \hat{R}(a_{\text{sing}})$ from the domain where $\hat{R} > \hat{R}_{\text{sing}} = \hat{R}(a_{\text{sing}})$. In the right panel, points 5 and 6 represent points where the right and left side of the phase space is sewn (some trajectories pass through the sewn singularity–points 5 and 6). Note that oscillating models exist (blue trajectory) and are situated around critical point 2. They represent oscillating models without the initial and final singularities. The green line represents the separatrix trajectory, which represents the only case for which the trajectory can pass from the left side of the phase portrait to the right one without the appearance of the sewn freeze singularity during the evolution. It joins saddle points in a circle at infinity. This line separates trajectories going to the freeze singularity from the bouncing solutions. For this case $\Omega_{\text{k}} = -\Omega_\gamma(\Omega_{\text{m},0}a^{-3} + 4\Omega_{\Lambda,0})^2\frac{(K-3)(K+1)}{2b} - (\Omega_{\text{m},0}a^{-3} + 4\Omega_{\Lambda,0})$ when $a = a_{\text{sing}}$.

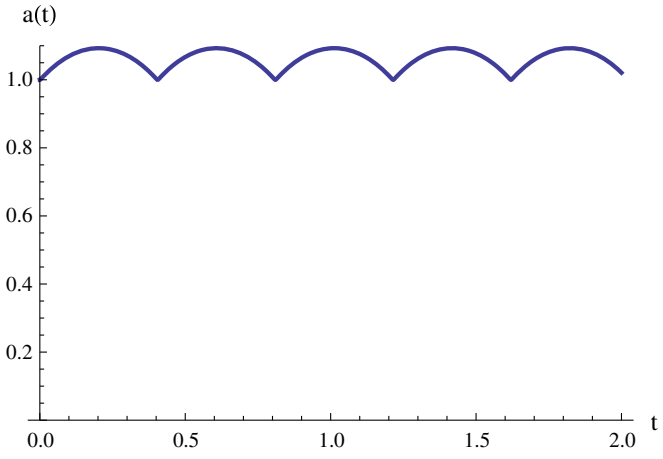

FIG. 13. The diagram presents the evolution of the scale factor for the trajectory of the oscillating orbit in the neighborhood of critical point 2 (see Fig. 12). The cosmological time is expressed in $\frac{\mathrm{s\,Mpc}}{100\ \mathrm{km}}$. Here, $a_{\min} = 1$.

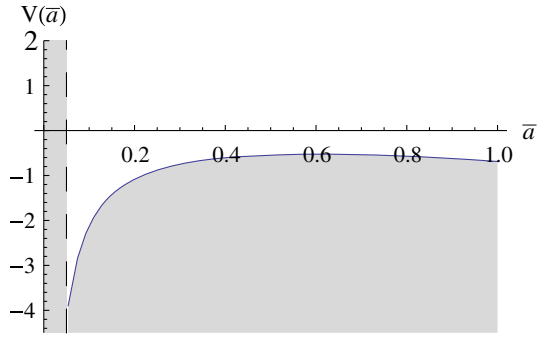

FIG. 14. The potential $V(\bar{a})$ for the Palatini formalism in the Einstein frame. The value of the parameter γ is chosen as $10^{-9}\,\frac{\mathrm{s^2\,Mpc^2}}{\mathrm{km^2}}$. The values of the $V(\bar{a})$ are given in $\frac{10^4\ \mathrm{km^2}}{\mathrm{s^2\,Mpc^2}}$. The dashed line represents the generalized sudden singularity. The value of the potential at the singularity is finite.

$$\bar{a} = \sqrt{\frac{C_0(1+2\gamma\hat{R}(\bar{t}))}{e^{-\frac{\arctan\left(\frac{-1+16\gamma\Lambda+32\gamma^2\Lambda\hat{R}(\bar{t})}{\sqrt{-1+32\gamma\Lambda}}\right)}{\sqrt[3]{-1+32\gamma\Lambda}}}\sqrt{4\Lambda+\hat{R}(\bar{t})(-1+16\gamma\Lambda+16\gamma^2\Lambda\hat{R}(\bar{t}))}}}, \tag{50}$$

where $C_0 = \frac{\bar{a}_0^2 e^{-\frac{\arctan\left(\frac{-1+16\gamma\Lambda+32\gamma^2\Lambda\hat{R}(\bar{t}_0)}{\sqrt{-1+32\gamma\Lambda}}\right)}{\sqrt[3]{-1+32\gamma\Lambda}}}\sqrt{4\Lambda+\hat{R}(\bar{t}_0)(-1+16\gamma\Lambda+16\gamma^2\Lambda\hat{R}(\bar{t}_0))}}{(1+2\gamma\hat{R}(\bar{t}_0))}$ with $\bar{a}_0$ as the present value of the scale factor, we get the first integral in the following form:

$$\bar{H}(\bar{t})^2 + \Lambda - \frac{\hat{R}(\bar{t})(2+\gamma\hat{R}(\bar{t}))}{6(1+2\gamma\hat{R}(\bar{t}))^2} + k\frac{e^{-\frac{\arctan\left(\frac{-1+16\gamma\Lambda+32\gamma^2\Lambda\hat{R}(\bar{t})}{\sqrt{-1+32\gamma\Lambda}}\right)}{\sqrt[3]{-1+32\gamma\Lambda}}}\sqrt{4\Lambda+\hat{R}(\bar{t})(-1+16\gamma\Lambda+16\gamma^2\Lambda\hat{R}(\bar{t}))}}{C_0(1+2\gamma\hat{R}(\bar{t}))} = 0. \tag{51}$$

As a result, the potential $V(\hat{R})$ is given by

$$V(\hat{R}) = \frac{a^2}{2}\left(\Lambda - \frac{\hat{R}(\bar{t})(2+\gamma\hat{R}(\bar{t}))}{6(1+2\gamma\hat{R}(\bar{t}))^2}\right). \tag{52}$$

Because we know the form of $V(\hat{R})$ and $\bar{a}(\hat{R})$, we can get the potential $V(\bar{a})$ in a numerical way. $V(\bar{a})$ potential is demonstrated in Fig. 14.

Equations (45)–(46) have the following first integral given by

$$H(t)^2 - \frac{(1+2\gamma\hat{R}(t))^2\left(-3\Lambda+\hat{R}(t) - \frac{k(-4\Lambda+\hat{R}(t))^{2/3}}{C_0} + \frac{\gamma(12\Lambda-3\hat{R}(t))\hat{R}(t)}{2(1+2\gamma\hat{R}(t))}\right)}{(1+2\gamma\hat{R}(t)-3\gamma(-4\Lambda+\hat{R}(t)))^2} = 0, \tag{53}$$

where $C_0 = a_0^2(-4\Lambda+\hat{R}(t_0))^{2/3}$. Here, a_0 is the present value of the scale factor.

VI. CONCLUSIONS

In this paper, the main conclusion is that the Starobinsky models in the Palatini formalism in the Jordan and Einstein frames are not physically equivalent. There are a few qualitative differences between the models in these frames. The most important difference is that the sewn freeze singularity in the Jordan frame is replaced by the generalized sudden singularity in the Einstein frame. Other differences between these frames are the lack of the big bang in our model in the Einstein frame and the fact that

phase portraits in these frames are not qualitatively equivalent. It is consistent with results obtained that models in the Jordan frame are not physically equivalent to those in the Einstein frame [75–79].

From the detailed analysis of cosmological dynamics in the Palatini formulation we derive the following conclusions:

(1) If we consider the cosmic evolution in the Einstein frame we obtain inflation as an endogenous effect from the dynamical formulation in the Palatini formalism [74].
(2) If we consider the cosmic evolution in the Jordan frame we obtain an exact and covariant formula for the variability of the gravitational constant G_{eff} parametrized by the Ricci scalar.
(3) Given two representations of our model in the Einstein and Jordan frames, we found that its dynamics are simpler in the Einstein frame as being free from some obstacles related to an appearance of bad singularities. It is an argument for the choice of the Einstein frame as physical.
(4) In our model considered in the Einstein frame, we have both the inflation as well as the acceleration [74]. While the inflation in the model is obtained as an inherited dynamical effect, the acceleration is driven by the cosmological constant term.
(5) In the model under consideration, we include effects of matter. This enables us to study the fragility of the inflation with respect to small changes of the energy density of matter [74].
(6) In the obtained evolutional scenario of the evolution of the Universe in the Einstein frame in the Palatini formalism we found the singularity of the finite scale factor (generalized sudden singularity) and the phase of the acceleration of the current Universe. Note that in [74] it was found the inflation in this model with the sufficient number of e-folds in the case when the matter is negligible.
(7) In the context of the Starobinsky model in the Palatini formalism we found a new type of double singularities beyond the well-known classification of isolated singularities.
(8) The phase portrait for the Starobinsky model in the Palatini formalism with a positive value of γ is equivalent to the phase portrait of the ΛCDM model. There is only a quantitative difference related to the presence of the nonisolated freeze singularity.
(9) For the Starobinsky-Palatini model in the Einstein frame for the positive parameter γ, a sewn freeze singularity is replaced by a generalized sudden singularity. As a result, this model is not equivalent to the phase portrait of the ΛCDM model.

ACKNOWLEDGMENTS

We are very grateful to A. Borowiec and A. Krawiec for stimulating discussion and remarks as well as to the anonymous referee for valuable comments.

[1] T. P. Sotiriou and V. Faraoni, Rev. Mod. Phys. **82**, 451 (2010).
[2] V. F. Mukhanov and G. V. Chibisov, JETP Lett. **33**, 532 (1981).
[3] A. A. Starobinsky, Sov. Astron. Lett. **9**, 302 (1983).
[4] P. A. R. Ade *et al.* (Planck), Astron. Astrophys. **594**, A14 (2016).
[5] C. Cheng, Q.-G. Huang, and Y.-Z. Ma, J. Cosmol. Astropart. Phys. 07 (2013) 018.
[6] Q.-G. Huang, J. Cosmol. Astropart. Phys. 02 (2014) 035.
[7] L. A. Kofman, A. D. Linde, and A. A. Starobinsky, Phys. Lett. **157B**, 361 (1985).
[8] S. V. Ketov and A. A. Starobinsky, Phys. Rev. D **83**, 063512 (2011).
[9] S. A. Appleby, R. A. Battye, and A. A. Starobinsky, J. Cosmol. Astropart. Phys. 06 (2010) 005.
[10] S. Capozziello, M. De Laurentis, S. Nojiri, and S. D. Odintsov, Phys. Rev. D **79**, 124007 (2009).
[11] A. Alho, S. Carloni, and C. Uggla, J. Cosmol. Astropart. Phys. 08 (2016) 064.
[12] S. Capozziello, M. F. De Laurentis, L. Fatibene, M. Ferraris, and S. Garruto, SIGMA **12**, 006 (2016).
[13] S. Capozziello, P. Martin-Moruno, and C. Rubano, Phys. Lett. B **689**, 117 (2010).
[14] S. M. Carroll, A. De Felice, V. Duvvuri, D. A. Easson, M. Trodden, and M. S. Turner, Phys. Rev. D **71**, 063513 (2005).
[15] M. Borunda, B. Janssen, and M. Bastero-Gil, J. Cosmol. Astropart. Phys. 11 (2008) 008.
[16] G. J. Olmo, Int. J. Mod. Phys. D **20**, 413 (2011).
[17] M. Ferraris, M. Francaviglia, and I. Volovich, Classical Quantum Gravity **11**, 1505 (1994).
[18] G. J. Olmo, Phys. Rev. D **72**, 083505 (2005).
[19] G. J. Olmo, Phys. Rev. Lett. **95**, 261102 (2005).
[20] C. Barragan and G. J. Olmo, Phys. Rev. D **82**, 084015 (2010).
[21] C. Barragan, G. J. Olmo, and H. Sanchis-Alepuz, Phys. Rev. D **80**, 024016 (2009).
[22] C. Bejarano, G. J. Olmo, and D. Rubiera-Garcia, Phys. Rev. D **95**, 064043 (2017).
[23] C. Bambi, A. Cardenas-Avendano, G. J. Olmo, and D. Rubiera-Garcia, Phys. Rev. D **93**, 064016 (2016).
[24] G. J. Olmo and D. Rubiera-Garcia, Universe **1**, 173 (2015).
[25] G. J. Olmo and D. Rubiera-Garcia, Eur. Phys. J. C **72**, 2098 (2012).

[26] G. J. Olmo and D. Rubiera-Garcia, Phys. Rev. D **84**, 124059 (2011).
[27] E. E. Flanagan, Phys. Rev. Lett. **92**, 071101 (2004).
[28] E. E. Flanagan, Classical Quantum Gravity **21**, 3817 (2004).
[29] F. A. T. Pannia, F. García, S. E. P. Bergliaffa, M. Orellana, and G. E. Romero, Gen. Relativ. Gravit. **49**, 25 (2017).
[30] H. Weyl, Ann. Phys. (Berlin) **364**, 101 (1919); **364**, 101 (1919).
[31] L. Page, Phys. Rev. **49**, 254 (1936).
[32] L. Page and N. I. Adams, Phys. Rev. **49**, 466 (1936).
[33] L. Page, Phys. Rev. **49**, 946 (1936).
[34] V. Canuto, P. J. Adams, S. H. Hsieh, and E. Tsiang, Phys. Rev. D **16**, 1643 (1977).
[35] T. Koivisto, Classical Quantum Gravity **23**, 4289 (2006).
[36] A. De Felice and S. Tsujikawa, Living Rev. Relativity **13**, 3 (2010).
[37] G. J. Olmo, Phys. Rev. D **75**, 023511 (2007).
[38] V. Faraoni, Phys. Rev. D **74**, 023529 (2006).
[39] M. Szydlowski, A. Stachowski, and A. Borowiec, Eur. Phys. J. C **77**, 603 (2017).
[40] A. Borowiec, M. Kamionka, A. Kurek, and M. Szydlowski, J. Cosmol. Astropart. Phys. 02 (2012) 027.
[41] L. Perko, *Differential Equations and Dynamical Systems*, 3rd ed., Texts in Applied Mathematics Vol. 7 (Springer, New York, 2001).
[42] A. Stachowski and M. Szydlowski, Eur. Phys. J. C **76**, 606 (2016).
[43] M. Szydlowski, A. Stachowski, A. Borowiec, and A. Wojnar, Eur. Phys. J. C **76**, 567 (2016).
[44] A. V. Yurov, A. V. Astashenok, and V. A. Yurov, arXiv:1710.05796.
[45] S. Nojiri, S. D. Odintsov, and S. Tsujikawa, Phys. Rev. D **71**, 063004 (2005).
[46] L. Fernandez-Jambrina, Phys. Rev. D **90**, 064014 (2014).
[47] R. R. Caldwell, M. Kamionkowski, and N. N. Weinberg, Phys. Rev. Lett. **91**, 071301 (2003).
[48] L. Fernandez-Jambrina and R. Lazkoz, Phys. Rev. D **74**, 064030 (2006).
[49] J. D. Barrow, Classical Quantum Gravity **21**, L79 (2004).
[50] J. D. Barrow, Classical Quantum Gravity **21**, 5619 (2004).
[51] J. D. Barrow, G. J. Galloway, and F. J. Tipler, Mon. Not. R. Astron. Soc. **223**, 835 (1986).
[52] M. Bouhmadi-Lopez, P. F. Gonzalez-Diaz, and P. Martin-Moruno, Phys. Lett. B **659**, 1 (2008).
[53] M. P. Dabrowski, K. Marosek, and A. Balcerzak, Mem. Soc. Ast. It. **85**, 44 (2014).
[54] M. P. Dabrowski and T. Denkiewicz, Phys. Rev. D **79**, 063521 (2009).
[55] M. P. Dabrowski and T. Denkiewicz, AIP Conf. Proc. **1241**, 561 (2010).
[56] L. Fernandez-Jambrina, Phys. Lett. B **656**, 9 (2007).
[57] A. Krolak, Classical Quantum Gravity **3**, 267 (1986).
[58] G. Allemandi, A. Borowiec, and M. Francaviglia, Phys. Rev. D **70**, 103503 (2004).
[59] J. Sbierski, J. Diff. Geom. **108**, 319 (2018).
[60] G. Galloway and E. Ling, Ann. Henri Poincare **18**, 3427 (2017).
[61] G. J. Galloway, E. Ling, and J. Sbierski, arXiv:1704.00353 [Commun. Math. Phys. (to be published)].
[62] E. Ling, arXiv:1706.01408.
[63] J. Sbierski, J. Phys. Conf. Ser. **968**, 012012 (2018).
[64] A. Stachowski, M. Szydlowski, and A. Borowiec, Eur. Phys. J. C **77**, 406 (2017).
[65] M. P. Dabrowski, arXiv:1407.4851.
[66] O. Hrycyna and M. Szydlowski, J. Cosmol. Astropart. Phys. 04 (2009) 026.
[67] G. F. R. Ellis, E. Platts, D. Sloan, and A. Weltman, J. Cosmol. Astropart. Phys. 04 (2016) 026.
[68] S. Weinberg, *Gravitation and Cosmology* (John Wiley and Sons, New York, 1972), ISBN 9780471925675.
[69] J. B. Jimenez, L. Heisenberg, and G. J. Olmo, J. Cosmol. Astropart. Phys. 06 (2015) 026.
[70] D. Bazeia, L. Losano, R. Menezes, G. J. Olmo, and D. Rubiera-Garcia, Classical Quantum Gravity **32**, 215011 (2015).
[71] V. Faraoni, E. Gunzig, and P. Nardone, Fund. Cosmic Phys. **20**, 121 (1999).
[72] H. Azri, arXiv:1802.01247.
[73] M. P. Dabrowski, J. Garecki, and D. B. Blaschke, Ann. Phys. (Berlin) **18**, 13 (2009).
[74] M. Szydlowski and A. Stachowski, Eur. Phys. J. C **78**, 249 (2018).
[75] S. Bahamonde, S. D. Odintsov, V. K. Oikonomou, and P. V. Tretyakov, Phys. Lett. B **766**, 225 (2017).
[76] S. Capozziello, M. De Laurentis, R. Farinelli, and S. D. Odintsov, Phys. Rev. D **93**, 023501 (2016).
[77] S. D. Odintsov and V. K. Oikonomou, Int. J. Mod. Phys. D **26**, 1750085 (2017).
[78] S. Bahamonde, S. D. Odintsov, V. K. Oikonomou, and M. Wright, Ann. Phys. (Amsterdam) **373**, 96 (2016).
[79] S. Capozziello, S. Nojiri, S. D. Odintsov, and A. Troisi, Phys. Lett. B **639**, 135 (2006).